CONDENSED MATTER PHYSICS

Conference materials
UDC 539.23+537.32+536.21
DOI: https://doi.org/10.18721/JPM.184.101

Si-Fe composites with embedded α-$FeSi_2$ nanocrystals: formation and thermoelectric properties

K.N. Galkin, O.V. Kropachev, O.A. Goroshko,
E.Yu. Subbotin, D.L. Goroshko, N.G. Galkin ✉

Institute of Automation and Control Processes, FEB RAS, Vladivostok, Russia
✉ galkin@iacp.dvo.ru

Abstract. The technology of embedding metallic iron disilicide (α-$FeSi_2$) nanocrystals (NCs) with different numbers of NCs multilayers and different doping levels of silicon multilayers with holes (10^{19} cm^{-3} and 10^{13} cm^{-3}) was tested on SOI substrates, and composites with 4 and 8 layers of embedded α-$FeSi_2$ NCs were grown using it. The maximum power factor 0.1 to 0.25 mW/(m×K²) at T = 450 K was observed in the composite with the maximum hole concentration in the silicon interlayers, and a decrease in the hole concentration led to a decrease in the power factor to 0.01 mW/(m×K²) at T = 450 K due to a sharp decrease in the sheet resistance with a weak increase in the Seebeck coefficient.

Keywords: silicon, α-$FeSi_2$ nanocrystals, crystal structure, doping, Si interlayers, conductivity, thermoelectric properties, power factor

Funding: The work was carried out with the support of the state assignment of the IACP FEB RAS FWFW-2006-0008

Citation: Galkin K.N., Kropachev O.V., Goroshko O.A., Subbotin E.Yu., Goroshko D.L., Galkin N.G., Si-Fe composites with embedded α-$FeSi_2$ nanocrystals: formation and thermoelectric properties, St. Petersburg State Polytechnical University Journal. Physics and Mathematics. 18 (4.1) (2025) 9–14. DOI: https://doi.org/10.18721/JPM.184.101

Материалы конференции
УДК 539.23+537.32+536.21
DOI: https://doi.org/10.18721/JPM.184.101

Композиты Si-Fe со встроенными нанокристаллами α-$FeSi_2$: формирование и термоэлектрические свойства

К.Н. Галкин, О.В. Кропачев, О.А. Горошко,
Е.Ю. Субботин, Д.Л. Горошко, Н.Г. Галкин ✉

Институт автоматики и процессов управления ДВО РАН, г. Владивосток, Россия
✉ galkin@iacp.dvo.ru

Аннотация. На подложках КНИ апробирована технология встраивания нанокристаллов (НК) металлического дисилицида железа (α-$FeSi_2$) с разным количеством мультислоев НК и разным уровнем легирования кремниевых мультислоев дырками (10^{19} $см^{-3}$ и 10^{13} $см^{-3}$) и по данной технологии выращены композиты с 4 и 8 слоями встроенных в кремний НК α-$FeSi_2$. Максимальный фактор мощности от 0.1 до 0,25 мВт/(м×K²) при T = 450 K наблюдался в композите с максимальной концентрацией дырок в кремниевых прослойках, а уменьшение концентрации дырок приводило к уменьшению фактора мощности до 0,01 мВт/(м×K²) при T = 450 K за счет резкого уменьшения слоевого сопротивления при слабом росте коэффициента Зеебека.

Ключевые слова: кремний, нанокристаллы α-$FeSi_2$, кристаллическая структура, легирование, прослойки Si, проводимость, термоэлектрические свойства, коэффициент мощности

Финансирование: Работа выполнена при поддержке государственного задания ИАПУ ДВО РАН (Тема FWFW-2026-0008).

Ссылка при цитировании: Галкин К.Н., Кропачев О.В., Горошко О.А., Субботин Е.Ю., Горошко Д.Л., Галкин Н.Г. Композиты Si-Fe со встроенными нанокристаллами α-$FeSi_2$: формирование и термоэлектрические свойства // Научно-технические ведомости СПбГПУ. Физико-математические науки. 2025. Т. 18. № 4.1. С. 9–14. DOI: https://doi.org/10.18721/JPM.184.101

Introduction

One of the approaches to creating efficient thermoelectric materials is to embed metal nanocrystals (NCs) into a semiconductor, such as germanium, which provides high matrix conductivity and an increase in the Seebeck coefficient [1]. It does not require high crystalline quality of materials with embedded nanocrystals and assumes the possibility of their random distribution in the semiconductor matrix, including silicon. NCs of transition metal silicides can be embedded into silicon, since they include both semiconductors [2] and metals [3]. It was known that embedding multilayers with one or two types of embedded NCs ($CrSi_2$ and β-$FeSi_2$) grown on an *n*-type silicon substrate resulted in efficient hole injection from embedded NCs, a change in the sign of the Seebeck coefficient from negative to positive, and an increase in the power factor in the temperature range from 200 K to 400 K [4]. At the same time, the incorporation of NC metal silicides into a silicon matrix with *p*-type conductivity and orientation (100), as well as the effect of doping silicon interlayers during the growth of multilayers on their thermoelectric parameters, remained unexplored.

In this paper, we investigated the formation of multilayers with embedded NCs of metallic iron disilicide (α-$FeSi_2$) in silicon-on-insulator (SOI) substrates of *p*-type conductivity with different numbers of NC multilayers and different doping levels of silicon multilayers, determined the phonon structure of the NCs, the conductivity and thermoelectric properties of the grown heterostructures in the temperature range of 80–450 K.

Materials and Methods

Multilayer heterostructures with embedded NCs of metallic α-$FeSi_2$ were grown in a VARIAN ultrahigh vacuum setup with a base pressure of 2×10^{-10} Torr equipped with a molecular beam source of iron (Fe), sublimation sources of silicon (Si) with different hole concentrations (p^+ and p^-) and a quartz thickness sensor. SOI Si(100) *p*-type wafers with a resistivity of (1–10) Ω × cm were chosen as substrates and Si sources. After low-temperature cleaning of the silicon surface at a temperature of 900 °C for 10 minutes, a 50 nm thick silicon buffer layer was deposited at $T = 700$ °C. Then, multilayer samples with embedded NCs of α-$FeSi_2$ were formed. This process consisted of four steps: (1) deposition of 0.5 nm Fe at room temperature; (2) annealing at $T = 630$ °C for 2 min and flash at $T = 1000$ °C for 5 s; (4) growth of the silicon layer (12 nm at $T = 630$ °C and 24 nm at $T = 700$ °C). To form 4-layer and 8-layer structures with embedded α-$FeSi_2$ NCs, these four steps were repeated 3 or 7 times, followed by growth of the capping silicon layer in two steps: 12 nm at $T = 630$ °C and 84 nm at $T = 700$ °C. Individual multilayers were grown with doped silicon interlayers with different hole doping: 10^{19} cm^{-3} (p^+) and 10^{13} cm^{-3} (p^-). For comparison with samples with embedded multilayers of α-$FeSi_2$ NCs, test samples were grown with 4 and 8 fictitious stages of silicon growth without deposition of iron atoms, but with annealing and stops (NC growth emulation or dummy composite (CS)) with different silicon sources (p^+ and p^-). A total of 3 samples with embedded α-$FeSi_2$ NCs and 3 samples with dummy CS were grown.

The morphology of the grown samples was studied using a Solver P47 scanning probe microscope in the tapping mode. The phonon structure of the grown samples was studied using an NTEGRA SPECTRA-II system in the Raman spectroscopy mode. The transport and thermoelectric properties of the samples were studied on a Kriotel (Russia) laboratory setup in a nitrogen atmosphere at temperatures of 80–450 K after preliminary formation of six Al contacts on an ADVAVAC PVD-2EB2R11 vacuum setup (To = 450 °C for 20 minutes) to measure conductivity and thermo-emf.

Results and Discussion

After unloading the samples with embedded α-$FeSi_2$ NCs and the reference samples with growth emulation, their surface morphology was studied by AFM. Due to the embedding of nanocrystals with a tetragonal lattice into silicon, a process of three-dimensional overgrowth of Si atop α-$FeSi_2$ NCs was observed and punctures were formed on the surface of the capping silicon layer. However, the yield of α-$FeSi_2$ NCs onto the surface of the composite was not observed. The root-mean-square roughness was minimal for 4-layer heterostructures both with embedded NC and without them (Table). Increasing the number of multilayers led to its 2–3-fold growth, but the depth of the observed punctures did not exceed 40 nm, which is less than the thickness of the capping silicon layer.

Table

Types of composites (CS), type of doping of Si interlayers, d_{CS} is total thickness of composite, σ_{rms} is root mean square roughness

Sample	Type of composite	Si interlayer doping	D_{CS}, nm	s_{rms}, nm
A	Dummy CS_1	p^+	256	2.0
B	4L α-$FeSi_2$	p^+	258	2.3
C	Dummy CS_2	p^+	375	7.0
D	8L α-$FeSi_2$	p^+	371	4.6
E	Dummy CS_3	p^-	417	0.51
F	8L α-$FeSi_2$	p^-	429	7.92

The study of the phonon structure of working samples by the Raman scattering method showed that multilayers with the supposed NC α-$FeSi_2$ do not have phonon peaks. This proves the absence of the semiconductor phase β-$FeSi_2$ [4] in the NC samples and indirectly confirms the formation of the α-$FeSi_2$ phase, which does not have resolved Raman scattering phonons [5].

The grown multilayer samples with embedded NCs (Table) represent a composite with randomly distributed NCs [4], to which the two-layer thermoelectric model [6] cannot be applied to isolate the contribution of the modified layer. The electrical and thermoelectric properties were analyzed by comparing the temperature dependences of the sheet resistance and the Seebeck coefficient for the SOI substrate, the emulated substrate (Dummy CS), and samples with embedded NCs. The data on the sheet resistance (Fig. 1, *a*) and the Seebeck coefficient (Fig. 1, *b*) were obtained for the SOI substrate and sample B with 4 layers of α-$FeSi_2$ NCs and the Dummy CS_1 (sample *A*), grown with heavily doped silicon interlayers (p^+). According to the sheet resistance dependencies, it was found that it is maximum for a clean SOI substrate (40 kW/□ at 320 K. At the same time, for embedded NCs or the Dummy CS Si sample, the sheet resistance decreases by 3–6 times depending on the temperature, so the doping of the intermediate silicon layers is strongly felt in the sheet resistance. The positive Seebeck coefficient for sample *B* with embedded NCs α-$FeSi_2$ increases from 360 μV/K at T = 80 K, reaches a maximum of 760 μV/K at T = 330 K and then saturates to 450 K (Fig. 1, *b*), which indicates the main contribution of holes. Sample *A* (Dummy CS_1) demonstrates an almost linear dependence of the Seebeck coefficient on temperature, increasing from +100 to +550 μV/K. That is, the incorporation of α-$FeSi_2$ NCs into the silicon composite leads to a sharp increase in the thermal generation of holes in the system compared to sample *A* (Dummy CS_1). For the SOI substrate with *p*-type conductivity, the large maximum

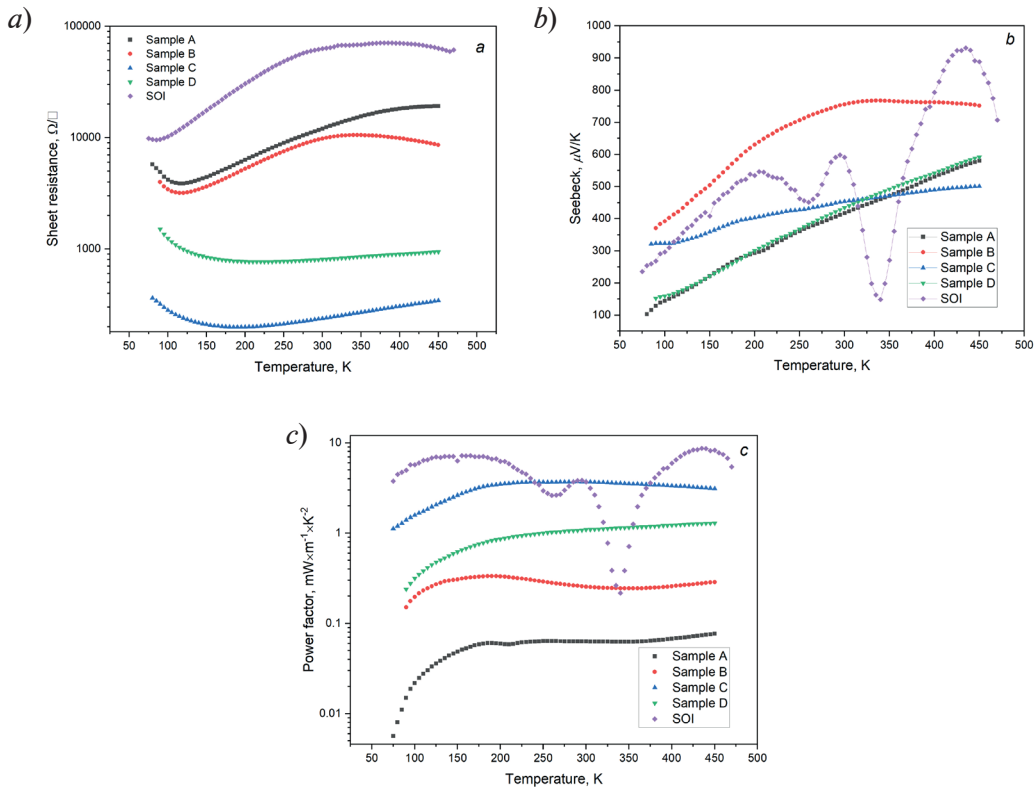

Fig. 1. Temperature dependences of the measured sheet resistance (*a*), Seebeck coefficient (*b*) and power factor (*c*) for the SOI-substrate, dummy CS_1 (samples *A*) and dummy CS_2 (sample *C*) and 4-layer an 8-layer composites in samples *B* and *D* with embedded α-$FeSi_2$ NCs respectively. The case of p^+ Si interlayer doping

(480 mV/K) for the Seebeck coefficient is observed at $T = 260$ K (Fig. 1, *b*), so the type of temperature dependences between substrate and grown samples are different. Calculations of the power factor showed (Fig. 1, *c*), that it remains minimal for sample *A* (Dummy CS_1), reaching 0.005 mW/(m×K^2) in the temperature range of 150–450 K. However, for sample *B*, the power factor reaches 0.02 mW/(m×K^2) at $T = 180$–450 K due to a higher sheet resistance and a lower Seebeck coefficient.

Doping of silicon layers to p^+ has a noticeable effect on the 8-layer sample *D* with embedded NCs (Table) and on the sample *C* (Dummy CS_2) (Table). In this case, for the latter sample, the sheet resistance with increasing temperature is lower than for the first by (6−10) times (Fig. 1, *a*). According to the Seebeck coefficient, sample *C* demonstrates a similar behavior as sample *A* (Fig. 1, *b*). For the multilayer sample with NC α-$FeSi_2$ (sample *D*), a smooth increase in the Seebeck coefficient is observed from 360 μV/K at $T = 80$ K to 750 μV/K at $T = 350$–450 K. Calculations of the power factor showed that it remains maximum for the Dummy CS_2 sample (*C*, Table), reaching 0.25 mV/(m×K^2) at $T = 250$ K and then reaching saturation (Fig. 1, *c*). For sample *D* with embedded NC α-$FeSi_2$, the power factor increases quasi-linearly with increasing temperature, reaching 0.1 mV/(m×K^2) at $T = 450$ K. That is, an increase in the number of embedded nanocrystal layers led to an increase (by 3–5 times) in surface resistance compared to sample *C* (Dummy CS_2) due to an increase in scattering on defects. The growth of the Seebeck coefficient in sample *D* is associated with the injection of holes into the composite layer. But this did not compensate for the decrease in the power factor for it compared to the Dummy CS_2 sample.

To determine the effect of decreasing the doping level of silicon interlayers on the thermoelectric parameters, a multilayer sample (8 layers) with a reduced hole concentration (p^-) was grown (Table, sample *F*). For sample *E* (Dummy CS_3), the sheet resistance (5 kΩ/□) at $T = 300$ K was significantly lower than for the SOI substrate (70 kΩ/□) at $T = 360$ K (Fig. 2, *a*). For sample *F*, the nature of the temperature dependence of the sheet resistance changed significantly, demonstrating

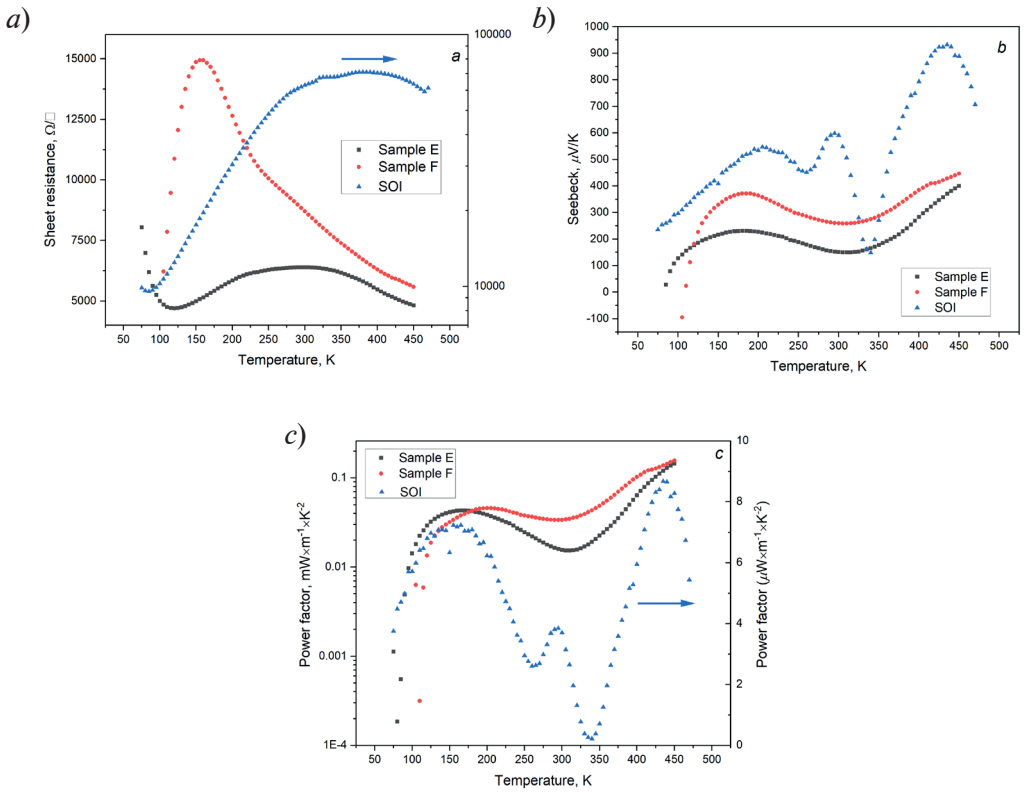

Fig. 2. Temperature dependences of the measured sheet resistance (*a*), Seebeck coefficient (*b*) and power factor (*c*) for the SOI-substrate, dummy CS_3 (sample *E*) and 8-layer composite in samples *F* with embedded α-$FeSi_2$ NCs. The case of p^- Si interlayer doping

a strong maximum (15 kΩ/□) at T = 160 K (Fig. 2, *a*). The difference in the behavior of the temperature dependences of the sheet resistance in samples *F* and *E* can be associated with a sharp increase in scattering on the built-in NCs compared to the multistep growth of silicon in the Dummy CS_3 sample. For the samples with embedded NC α-$FeSi_2$ (sample *F*) and sample *E* (Dummy CS_3), the Seebeck coefficient (Fig. 2, *b*) changes non-monotonically with temperature, but demonstrating a similar nature of the dependencies. Two maxima are observed for them, but the Seebeck coefficient is greater for sample *F*. The first maximum (370 μV/K for sample *F* and 220 μV/K for sample *E*) is observed at T = 160–180 K, and the second maximum (420 μV/K and 370 μV/K, respectively) at T = 450 K (Fig. 2, *b*). Calculation of the power factor from temperature for samples *E* and *F* and comparison with the SOI substrate showed that in the temperature range of 150–300 K, the most efficient thermoelectric is SOI substrate (0.1 mV/(m×K^2)). But with increasing temperature, the power factor for both samples (*E* and *F*) also increase, reaching a value of 0.01 mW/(m×K^2) at T = 450 K.

Conclusion

A comprehensive technology for embedding α-$FeSi_2$ NCs into SOI substrates has been developed using solid-phase epitaxy with different growth temperature modes (T = 630 °C and T = 1000 °C) for annealing 0.5 nm thick iron layers and molecular beam epitaxy (T = 630–700 °C) of Si interlayers. 4-layer and 8-layer samples with embedded α-$FeSi_2$ NCs and silicon interlayers (hole concentration: 10^{19} cm^{-3} and 10^{13} cm^{-3}), as well as multilayer samples with emulation of NC growth on SOI-(100) substrates have been grown. It was found that in the 8-layer heterostructure with the maximum hole concentration in the silicon interlayers, a sharp decrease in the sheet resistance is observed for the case of growth emulation compared to the incorporation of α-$FeSi_2$ NCs and some increase in the Seebeck coefficient at T = 80–35 K. This leads to an increase in the power factor to 0.25 mW/(m×K^2) for the sample with growth emulation and 0.1 mW/(m×K^2) for the sample with embedded α-$FeSi_2$ NCs at T = 200–450 K. A decrease in the hole concentration in silicon multilayers with embedded NC α-$FeSi_2$ leads

to both a decrease in the Seebeck coefficient and a decrease in the power factor (up to 0.01 mW/(m×K²) at $T = 450$ K due to a sharp increase in the sheet resistance during scattering at grain boundaries.

Acknowledgments

The study was carried out within the framework of the state assignment of the Institute of IACP FEB RAS (state budget topic FWFW-2026-0007).

REFERENCES

1. **Tanusilp S.,** Kurosaki K., Si-based materials for thermoelectric applications, Materials. 12 (2019) 1943.

2. **Murarka S.P.,** Silicide thin films and their applications in microelectronics, Intermetallics. 3 (3) (1995) 173–186.

3. Ed. by Borisenko V.E., Semiconducting Silicides (Berlin, Springer, 2000).

4. **Galkin N.G., Galkin K.N., Dotsenko S.A., Serhiienko I., Khovailo V.V., Gutakovskii A.K.,** Effect of embedding of $CrSi_2$ and β-$FeSi_2$ nanocrystals into *n*-type conductivity silicon on the transport and thermal generation of carriers, Applied Surface Science. 566 (2021) 150620.

5. **Pushkarev R.V., Fainer N.I., Katsui H., Kaichev V.V., Goto T.,** Structural features and surface composition of epitaxial α-$FeSi_2$ films obtained by CVD, Mater. Des. 137 (2018) 422–429.

6. **Bahk J.H., Favaloro T., Shakouri A.,** Thin film thermoelectric characterization techniques, Annual Review of Heat Transfer. 16 (2013) 51–99.

THE AUTHORS

GALKIN Konstantin N.
galkinkn@iacp.dvo.ru
ORCID: 0000-0001-5386-1013

SUBBOTIN Evgenii Yu.
jons712@mail.ru
ORCID: 0000-0001-9531-3867

KROPACHEV Oleg V.
chernobez@gmail.com
ORCID: 0000-0003-4300-0070

GOROSHKO Dmitrii L.
goroshko@iacp.dvo.ru
ORCID: 0000-0002-1250-3372

GOROSHKO Olga A.
olgagoroshko@iacp.dvo.ru
ORCID: 0009-0008-2152-140x

GALKIN Nikolay G.
galkin@iacp.dvo.ru
ORCID: 0000-0003-4127-2988

Received 12.09.2025. Approved after reviewing 20.11.2025. Accepted 08.12.2025.